Improving frequency containment reserve provision in run-of-river hydropower plants

F. Gerini [a],[*], E. Vagnoni [b], R. Cherkaoui [a], M. Paolone [a]

[a] Distributed Electrical Systems Laboratory, EPFL, Lausanne, Switzerland
[b] Technology Platform for Hydraulic Machines, EPFL, Lausanne, Switzerland

ARTICLE INFO

ABSTRACT

The paper presents a model-based control strategy for optimal asset management of hydroelectric units in run-of-river hydropower plants. The proposed control strategy aims to operate the unit at the best efficiency while improving water flow management and minimise components wear during frequency containment reserve provision. This approach is designed for a double regulated turbine (Kaplan) with adjustable guide vanes angle and runner blades angle and can be extended to other turbines adopted in run-of-river hydropower plants. The optimal discharge set-point is computed for maximising the frequency containment reserve provision while controlling the head of the river. The best efficiency is achieved by solving a suitably defined convex optimisation problem leveraging a regressive model of the hydraulic characteristics of the turbine and dynamics of the guide vanes and blades servomotors. The discharge set-point combines three terms: the dispatch plan set-point, the regulating discharge, proportional to the grid frequency deviation, and an offset term computed to control the average flow through the machine. Furthermore, a method to forecast the energy required in the following hour for the provision of grid frequency regulation is exploited to enhance the unit's frequency containment reserve action. The control strategy is validated by simulating a month of operation for the full-scale run-of-river hydropower plant located in Vogelgrun (France) and by comparing the results with operational statistics. Results show the effectiveness of the proposed control strategy able to increase the provision of frequency containment reserve while decreasing the number of movements of the machine components and maximise the efficiency.

1. Introduction

The need for integrating renewable energy sources in the European power mix has long been ascertained as a fundamental step of the decarbonisation process. Moving towards this direction raises multiple challenges for the electrical power system, not last the need for power balancing and flexibility services provision to mitigate the massive integration of non-dispatchable sources. Hydropower, as a dispatchable source, accounted in 2018 for 16.8% of the total electricity generated in the European interconnected transmission system [1]. In this regard, many studies in the literature, such as [2–4], indicate that hydropower shall be a key player in the ambitious high *Renewable Energy Sources* (RES) scenario by supporting the power grid balancing and extending the flexibility of the European power system. *Hydropower Plants* (HPPs) have been playing a major role in frequency regulation [5,6]. As volatile renewable sources continue to grow in number and generated power, HPP can support this evolution especially by contributing to the provision of Frequency Containment Reserve (FCR) [2]. Part of this reserve can be offered by *Run-of-River* (RoR) power plants, accounting for 5.93% of the total generated electricity in the ENTSOE area [7]. RoR HPPs are often equipped with double regulated machines (i.e. machines able to control guide vanes and blades opening angles), namely Kaplan turbines. These turbines are used thanks to their ability to guarantee high-efficiency values through a wide range of water discharge conditions. These power plants do not encounter the big disadvantage of having to deal with the water hammer phenomenon when providing fast regulation, a critical issue that affects long-penstock HPPs [8]. Nevertheless, some difficulties are encountered when providing flexibility with RoR HPPs. According to [9], enhancing frequency control actions of HPPs has a considerable effect on the wear and tear of the hydraulic and mechanic system. Furthermore, the need for tracking the discharge set-point with good accuracy assumes great importance in RoR HPPs [10,11]. This results from the necessity of complying with the day-ahead dispatch, and of controlling the river head for safety reasons. The increase of frequency control actions could enlarge the discrepancy between discharge set-point usually established by day-ahead markets and real value of the discharge.

Therefore, a flow management action is required to verify that the discharge deviation originated by the provision of frequency control is limited over time. Furthermore, for Kaplan turbines, continuous movements of the guide vanes and blades, due to both FCR provision and set-point compliance, increase the wear and tear of the mechanic and hydraulic components and, therefore, affect the turbine lifetime and performance [9]. In particular, the provision of FCR is responsible for: (i) (ii) an increase of wear and fatigue [9] and (iii) a decrease of the machine performance, especially in terms of efficiency [12] . [12] shows that the governor setting directly influences the efficiency loss: the higher the frequency droop, the greater the efficiency loss. Finally, [13] assess a relation between wear and blades vibration, which causes a decrease in the performance that can eventually lead to outages. Consequently, HPP owners are interested in reducing the FCR provision, to minimise the effect of wear and tear on their assets. In this direction, [14] proposes a dedicated setting of the PID parameters and the introduction of controller filters to partially reduce the reaction of hydropower units to frequency deviations. Similarly to [14], in most studies on the design and tuning of FCR controllers of hydropower units for the minimisation of wear and tear [15–19] are discussed. Nevertheless, to the best of the authors' knowledge, while the literature focuses on the governor settings, the formulation of control problems for the optimal discharge management of RoR HPP providing FCR and, at the same time, minimising the unit wear to increase lifetime and minimise maintenance, is not thoroughly addressed. Therefore, novel control strategies are required to optimise the asset management of RoR HPP while increasing the provision of FCR to enhance the flexibility of modern power systems. By targeting the fulfillment of this gap, this paper proposes a multilevel control strategy that embeds a discharge control framework capable to: (i) select the maximum frequency droop that allows the HPP to operate while respecting the discharge set-point, (ii) contain the discharge error during operation, and At the same time, the proposed framework targets efficiency maximisation for the HPP. Furthermore, the paper presents a novel real-time control formulated as a convex optimisation problem to ensure time-efficient computation, as well as optimality and uniqueness of the determined control set-point. To achieve these features, the proposed approach uses an accurate method to model the behaviour of double-regulated hydro-turbines with analytical functions. The proposed methodology represents a leap in the digitalisation process of hydropower plant, and in the ability of supporting the power system flexibility with higher reliability.

The paper is organised as follows. In Section 2, the control problem is introduced. Section 3 describes the theoretical framework to obtain analytical functions modelling the machine characteristics. Section 4 presents the whole multilevel control strategy. The simulation results are discussed in Section 5.

2. Problem statement

According to [20], as of 2019, almost 42% of the turbines installed in Europe are double regulated turbines. Moreover, RoR power plants accounted for 217.1 TWh out of the total 3659.1 TWh production in 2018 in the ENTSOE area, corresponding to 16.7% of the total renewable generation [1]. For this reason, the objective of this study is the development of a control strategy to optimise the FCR provision of double-regulated turbines, typical machines deployed in low head hydropower plants. The proposed control is developed to provide technical solutions to the following points:

(A) Improve the hydropower plant FCR provision.

(B) Develop a discharge management framework capable to ensure the discharge set-point to be respected while minimising the HPP unit wear and tear.
(C) Exploit the full operating range of the hydro machine by taking into consideration guide vanes and blades as decoupled variables to achieve the maximum efficiency under any head condition.

2.1. Improving FCR provision

In droop-based frequency control systems, increasing the FCR provision means increasing the droop of the unit's primary frequency control. A way to calculate the highest value of frequency droop that can be achieved compatibly with the operational condition of the HPP, is proposed in Section 4.1. In particular, special attention is applied to the modelling of the relation between frequency-droop value and deviation of the realised discharge from its set-point.

2.2. Discharge management framework

The increase of the frequency droop coefficient, i.e. the increase of FCR provision, leads to two main problems: (i) increase of the wear and tear of the hydraulic and mechanic system of the HPP unit; (ii) difficulties in complying with the HPP discharge set-point. The discharge management frameworks proposed in this paper targets the mitigation of both problems. As explained in [9], in double regulated turbines, for both guide vanes and blades, the wear and tear phenomenon is mainly influenced by:

- the cumulative distance of movements L;
- the total amount of movement direction changes M.

Over a time period that includes M movements, the so-called *cumulative distance L* is defined by [9] as:

$$L = \sum_{m=1}^{M} d_m \tag{1}$$

where d_m is the distance of one single movement. A way to compute the number of movements M the distance of one movement d_m is shown in Fig. 1, where the number of movements is considered as the number of direction changes of the actuators controlling the opening of either guide vanes or blades. In RoR power plants, the two main factors contributing to the increase of guide vanes ad blades movements are: (i) FCR provision and (ii) discharge management. By enhancing FCR provision, the cumulative distance L increases. Working with a higher droop inevitably results in having longer movements d_m of guide vanes and blades, and, therefore, more wear and tear. Furthermore, the provision of FCR indirectly increases the number of movements of guide vanes and blades because it requires a discharge management system to compensate for the discharge deviations originated by FCR. This latter effect can be reduced by developing a control targeting the minimisation of the number of movements M originated by the discharge management while enhancing the FCR provision of the HPP. The development of this framework is shown in details in Section 4.2.

2.3. Exploiting the full HPP operating range

The optimal control is performed by decoupling the action of guide vanes and blades as an alternative to the general gate-based control [21], which has been proved to be a successful strategy in [22]. The standard operation of the Kaplan unit is considered, while start-up and stop procedures are not the objects of this study. Numerous studies [23–26] have shown that, for a
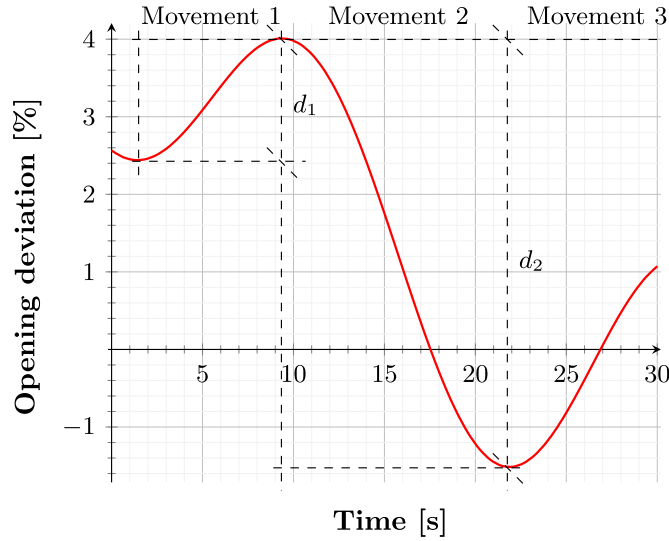
Fig. 1. Number of movements M and distance d_m according to [9] for a general trajectory of a moving organ (i.e guide vane or blade) expressed in terms of percentage opening deviation.

double-regulated turbine, the hydraulic machine efficiency η and discharge Q can be modelled as nonlinear functions of (i) guide vanes opening angle α, (ii) blades angle opening β, (iii) head H and (iv) rotational speed n:

$$\eta = \eta(\alpha, \beta, H, n) \tag{2}$$

$$Q = Q(\alpha, \beta, H, n) \tag{3}$$

where the quantity η is defined, as in [27], as the ratio between the supplied power and hydraulic power. Eqs. (2) and (3) represent the stationary behaviour of the turbine. Since RoR power plants are characterised either by the absence of a penstock or by the presence of a very short one, it is possible to neglect the turbine dynamic behaviour and consider (2) and (3) as representative of the hydraulic system. Given the analytic expressions for η and Q, knowing the head $\hat{H}$ and the rotational speed $\hat{n}$, the control problem can be written in the form:

$$\max_{\alpha, \beta} \quad \eta(\alpha, \beta, \hat{H}, \hat{n})$$
$$\text{s.t.} \quad Q^{SET} = Q(\alpha, \beta, \hat{H}, \hat{n}) \tag{4}$$
$$\alpha, \beta \in \Omega_{\alpha, \beta}$$

where Ω_α, Ω_β represent the sets of all feasible values of α and β respectively. The set-point given to the HPP is considered to be a set-point in discharge Q^{SET}, which is often the case for RoR power plants. In fact, the river head is usually monitored and controlled by dispatchers, who communicates the discharge set-point to the different HPPs. In the following section, (2) and (3) are rearranged to be suitable for the optimisation problem presented in Section 4.3.

3. Surrogate model of a Kaplan turbine performance

To model the turbine behaviour, and to compute the optimisation problem expressed by (4), it is necessary to build two analytical and continuous functions modelling the efficiency and the turbine discharge. With the scope of representing the turbine behaviour as a function of the controllable variables (i.e., α and β), it is possible to generalise the problem and reduce the number of variables in (2) and (3) by introducing the IEC speed coefficient

n_{ED}:

$$n_{ED} = \frac{nD}{\sqrt{gH}} \tag{5}$$

where D is the runner diameter and $g = 9.81$ m/s^2 the gravitational acceleration. The surrogate models of the efficiency η^* and the discharge Q^* are built as a function of α, β and n_{ED}.

$$\eta = \eta^*(\alpha, \beta, n_{ED}) \tag{6}$$

$$Q = Q^*(\alpha, \beta, n_{ED}) \tag{7}$$

For this purpose, the *Multivariate Adaptive Regression Spline* (MARS) technique [28] is employed. This technique is selected for its ability to fit (6) and (7) with analytical functions, continuous in their first derivative, which are particularly suitable to be used by optimisation frameworks. Furthermore, the MARS modelling allows for evaluating the influence of each independent variable by using only an initial exploration data-set which is well suited to validate the independent variables selected in this study. A similar approach can be found in [29,30]. Similarly to [30], the best function degree can be selected by performing a preliminary model considering all the parameters and evaluating the coefficient of determination (R^2) by changing the maximum function degree.

By considering a dependent variable y^* (i.e., η^* and Q^*) as a function of the independent variables $\boldsymbol{x}$ (i.e., α, β and n_{ED}), the MARS approximation is built as a linear statistical model:

$$y^* = f(\boldsymbol{x}, \gamma) = \gamma_0 + \sum_{m=1}^{M} \gamma_m \cdot B_m(\boldsymbol{x}) \tag{8}$$

where M is the number of independent basis functions and γ_m the unknown coefficient for the mth basis function. $B_m(\boldsymbol{x})$ denotes a specific base function which is built as a combination of univariate basis functions $b_m^\pm$ in the form of a truncated linear function:

$$b_m^+(x, t) = |x - t|_+ = \max(0, x - t)$$
$$b_m^-(x, t) = |t - x|_+ = \max(0, t - x) \tag{9}$$

where t is an univariate knot. From (9), each $B_m(\boldsymbol{x})$ is created by multiplying an existing basis function by a truncated linear function involving a new variable, as follows:

$$B_m(\boldsymbol{x}) = \prod_{l=1}^{L_m} \max(0, \pm(x_{v(l,m)} - t_{l,m})) \tag{10}$$

where L_m indicates the number of truncated linear functions multiplied in the mth basis function, $x_{v(l,m)}$ is the input variable corresponding to the lth truncated linear function, and $t_{l,m}$ is the knot value corresponding to $x_{v(l,m)}$. A forward step-wise algorithm, based on linear regression, selects the model basis functions, the corresponding coefficients and the appropriate knots. It is followed by a backward procedure to prune the model terms to eliminate over-fitting [28]. To train the algorithm, a data-set is collected using the original characteristic curves of the turbine and one-year operational statistics, as it will be further detailed in Section 5. The model fitting performances are evaluated by the *Mean Square Error* (MSE), by the *Coefficient of Determination* R^2, and by the *Generalised Cross Validation* error (GCV) computed as:

$$GCV = \frac{1}{N_{sp}} \frac{\sum_{j=1}^{N_{sp}} \left(y(^j\boldsymbol{x}) - y^*(^j\boldsymbol{x})\right)^2}{\left(1 - \frac{z_M}{N_{sp}}\right)} \tag{11}$$

where z_M is the number of MARS independent variables and N_{sp} the number of samples y in the data-set. Although this methodology allows for creating accurate models of efficiency
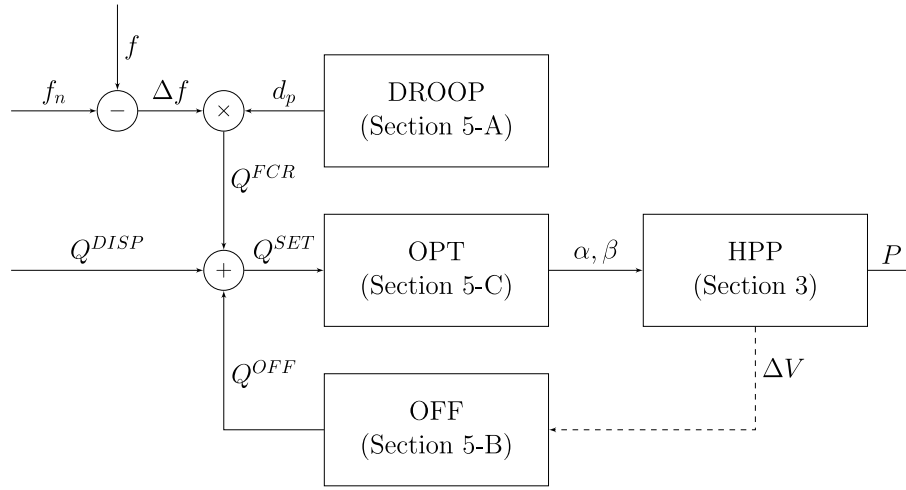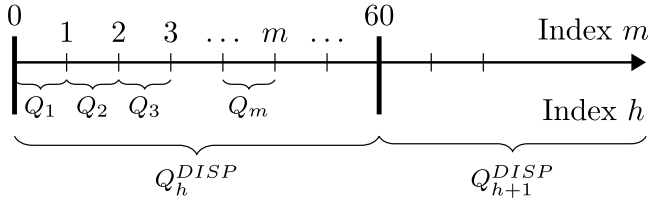
Fig. 2. Multilevel control strategy control diagram.

Fig. 3. Set-point problem on a time scale.

and discharge, it does not imply the convexity (nor the concavity) of the obtained η^* and Q^*. This is an important observation that has consequences on the optimisation problem computation discussed next, whose convexification is one the main paper contributions.

4. Multilevel control strategy

The control framework is composed of multiple layers, that are executing the computations on different time-horizons:

(A) Daily computation of the droop coefficient d_p (DROOP), accordingly with the usual market practice in most of the European countries[1]

(B) Hourly computation of the discharge offset term based on a forecast of the discharge required in the following period to perform FCR with the computed droop (OFF).

(C) Real-time control, by solving a convex optimisation problem taking into account the provision of FCR and having as input the sum of discharge set points and hourly offset (OPT).

The control diagram is presented in Fig. 2. The discharge set-point Q^{SET} fed into the optimisation problem is calculated by summing three contributions: (i) the original set-point given by the day-ahead dispatch plan Q^{DISP}; (ii)a droop-based frequency regulation originating a deviation from the main set-point Q^{FCR}; (iii) an offset discharge term, computed periodically, to ensure that the discharge deviation is contained within certain limits, chosen a priori to ensure the correct management of the river Q^{OFF}. The

HPP block refers to the power plant model and is considered as described by (6) and (7). The strategy is to be applied to RoR hydropower plants equipped with double regulating machines (i.e., Kaplan turbines). Nevertheless, by removing the latter level of the computation (OPT), the control can be extended to any kind of RoR hydropower plant equipped with other types of turbines. In this case, the obtained set point Q_{SET} is simply considered as the sole input of the governing system. The division of the control problem in different time horizons allows relaxing the constraints on the HPP set-points, therefore, adding a degree of freedom to the control problem. For instance, as shown in Fig. 3, a certain discharge set-point Q_h^{DISP}, coming from the dispatch plan, has to be respected over an hour h. The consequence, in an ordinary control system, is a control action that at every time step m, (i.e. each minute) imposes a discharge set-point Q_m equal to Q_h^{DISP}, for the entire hour, as follows:

$$Q_m \approx Q_h^{DISP} \quad \forall m \in [1, \ldots, 60] \tag{12}$$

Nevertheless, except for the case of extremely small rivers, the head is not a function of a single power plant discharge and it changes, generally very slowly, as a consequence of many external parameters. Therefore, there is no need for strictly applying (12) for the calculation of Q_m and the problem can be relaxed and expressed in its integral form:

$$\Delta V_h = \sum_{m=1}^{60} Q_m - 60 \cdot Q_h^{DISP} \approx 0 \tag{13}$$

where ΔV_h indicates the *Cumulative Discharge Error* (CDE), expressed in m^3 for the hour h. By imposing this latter to be equal to zero, (13) ensures the set-point request to be fulfilled at the end of every period (i.e. every hour). A further element of complexity is given by the discharge set-point which is modified due to FCR provision. Even if every minute m the set-point $Q_m = Q_h^{DISP}$ is fed into the control system, a deviation from the given set-point is always introduced by the FCR provision modifying the discharge through the hydraulic machine. Every hour h, the error accumulated ΔV_h is:

$$\Delta V_h = \Delta V_{h-1} + \Delta V_h^{FCR} \tag{14}$$

where: ΔV_{h-1} is the CDE of the previous hour and ΔV_h^{FCR} is the cumulative deviation due to FCR provision, in the hour h. The term ΔV_h^{FCR} is related to the energy E_h^{FCR}, required over the hour h to provide frequency control, as follows:

$$\Delta V_h^{FCR} = \frac{E_h^{FCR}}{K_h} \tag{15}$$

---

[1] The transmission system operators of Germany, France, Belgium, the Netherlands, Austria and Switzerland share frequency containment reserve on a common platform [31] on a daily base. The market for FCR-N is also based on day-ahead bidding in the Nordic countries [32].

Table 1
Residual standard deviation σ for $AR(0)$ and $AR(8)$.

T [h]	1	2	3	4
AR(0)	30	52	73	93
AR(8)	24	43	59	74

where K is a conversion factor between produced energy and amount of water flowing through the HPP.

$$K = \rho g H \eta \tag{16}$$

In (15) the terms K_h indicates the average value of K over the hour h. For a droop based FCR provision, the energy E^{FCR} can be computed as [33]:

$$E_h^{FCR} = d_p \int_T \Delta f dt = d_p W_f \tag{17}$$

where W_f is defined as the integral of the frequency deviation over time, T indicates the length of the interval (i.e. 1 h) and Δf indicates the deviation of the frequency from its nominal value. Eqs. (15) and (17) express the link between W_f and the amount of additional water (positive or negative) that has to flow through the turbine to provide FCR in a certain time period. The quantity W_f is supposed to be zero over a long time period T, if the *Frequency Restoration Reserve* (FRR) is well planned in the synchronous area (i.e. the Synchronous grid of Continental Europe in the case of the HPP of Vogelgrun). However, this is not verified for a shorter time window (i.e. if $T = 1$ h). If no action is taken, the discharge could deviate considerably from its expected value because of FCR provision, causing the alteration of the river head as well.

In order to optimise the discharge management, this study proposes to deploy a forecasting tool to obtain a prediction $\hat{W}_f$ of the quantity W_f. This tool has been proposed and analysed in [33] for the control of battery energy storage systems providing FCR. In [33], it is proved that *Auto-Regressive* (AR) models can be exploited to forecast W_f. In particular, the study shows that AR models of order 8 (i.e. AR(8)) are well suited for the scope. The AR(8) model used in this study has been trained with one-year-long (March 2019-March 2020) site frequency measurements at EPFL, Lausanne [34]. The residual standard deviations of frequency measurements, valid for the continental Europe synchronous area, are compared in Table 1 for different interval lengths. The forecasting tool has been tested on a set of one-month data (15-Apr-2020 to 15-May-2020). The prediction error $\hat{W}_f - W_f$ is compared to its confidence interval $1.96 \cdot \sigma_f$. By enforcing this confidence interval, the forecast targets a coverage of 95%. The validation over the data-set returns a coverage of 95.5%. By exploiting this forecasting tool, it is possible to predict W_f and, therefore, ΔV_h^{FCR} once the droop is fixed. Having information about W_f also allows deciding the maximum frequency droop and for computing the offset discharge term every hour. Fig. 4 shows the expected domain for $W_f(t)$ computed on the EPFL data-set and with $T = 1$ h.

4.1. Optimal Daily Droop Coefficient (DROOP)

As mentioned in Section 2, one of the objectives of the framework is the improvement of the hydropower regulation action. In droop-based frequency control, this can be done by augmenting the droop value. For this reason, this first block of the framework determines, on a daily basis, the optimal value of the droop coefficient as the one with the highest value and capable to satisfy the operational condition of the HPP. The choice is limited by two factors. The first limitation comes from the inevitable increase
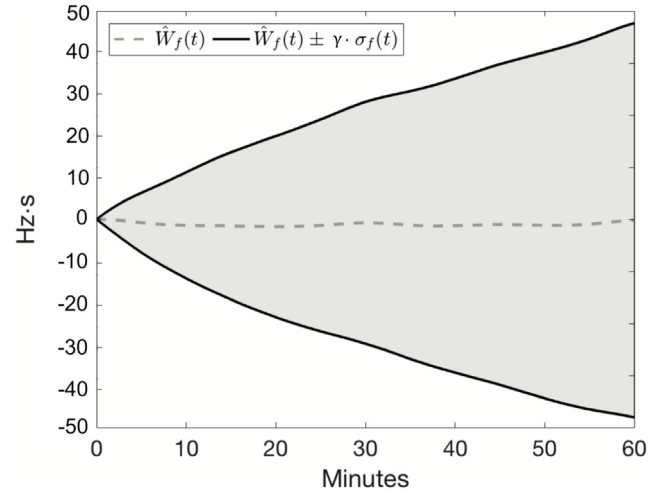

Fig. 4. In light grey, the confidence interval of the expected evolution of $W_f(t)$ in 1-hour time intervals, EPFL data-set [33], where $\gamma = 1.96$.

of the deviation of the HPP discharge from the discharge set-point due to the droop enhancement. Hence, it is necessary to accept a certain CDE ΔV_{max} and compute the maximum droop that allows respecting this condition. The second constraint is due to the power limitation of the hydraulic machine. If the turbine is already operating close to its maximum (or minimum) power, it could be impossible to perform FCR provision as requested. It is possible to map these two limitations in two constraints.

1. Maximum admissible CDE.
2. Maximum power of the machine.

Therefore, the problem of the droop computation can be divided into two sub-problems, each one giving a possible value of droop as output. Every day, the droop is calculated to be the minimum of these two values: d_p^D and d_p^P, respectively.

4.1.1. Maximum admissible CDE

Every hour h of the day d, considering a droop-based FCR action with droop equal to d_p^D, the term ΔV_h^{FCR} can be predicted starting from the prediction $\hat{W}_f$ and considering Eqs. (15) and (17) as follows:

$$\Delta V_h^{FCR} \in \left[\frac{d_p^D}{K_h} \left(\hat{W}_{f,h} - \gamma \sigma_f \right), \frac{d_p^D}{K_h} \left(\hat{W}_{f,h} + \gamma \sigma_f \right) \right] \tag{18}$$

where σ_f is the standard deviation of the $\hat{W}_{f,h}$ prediction of W_f for the hour h, $\gamma = 1.96$ is chosen to target a *Confidence Interval* (CI) equal to 95% and K_h indicates the average value of K over the hour h. The target of the discharge management is to introduce a water volume ΔV_h^{OFF} able to compensate for the effect of ΔV_h^{FCR} and for the CDE of the previous hour ΔV_{h-1}, as visible from (19):

$$\Delta V_{h-1} + \Delta V_h^{OFF} + \frac{d_p^D}{K_h} \hat{W}_{f,h} = 0 \tag{19}$$

If (19) is respected for every hour h of a day d, the maximum possible CDE depends only on the forecasting accuracy. In particular, once the maximum permitted cumulative discharge error ΔV_{max} is decided by the river authorities, or by the HPP owner, the maximum acceptable droop for the day d can be computed similarly to [35] by solving (20):

$$\Delta V_{max} = \gamma \sigma_f d_p^D / K_d \tag{20}$$

$$d_p^D = \frac{K_d \cdot \Delta V_{max}}{\gamma \cdot \sigma_f} \tag{21}$$

where K_d indicates the average value of K over the day d. The latter equation shows that having a lower σ_f on the forecast allows increasing the acceptable droop and the provision of FCR. Similarly, by allowing a bigger ΔV_{max}, an increase of FCR provision can be achieved. On the other side, ΔV_{max} is limited by river authorises.

4.1.2. Maximum power of the machine limitation

A second limitation on the droop is given by the maximum power of the machine. To ensure continuous operation, the droop has to be selected to comply with the maximum power capacity of the machine. This means that the power deviation caused by FCR provision plus the dispatch production $\hat{P}_h^{disp}$ for every hour h of the day d must not be greater than the maximum power capacity of the machine. This limitation is expressed for a day d by considering the maximum values of both the components in (22).

$$d_p^P = \frac{P_n - \left(\hat{P}_{max}^{DISP} + K_d \Delta V_{max}/2\Delta T\right)}{\Delta f_{max}} \qquad (22)$$

where P_n is the nominal power of the machine and $\hat{P}_{max}^{DISP}$ maximum value of the dispatched power over the day d, namely:

$$\hat{P}_{max}^{DISP} = \overset{24}{\underset{h=1}{\max}}\left(\hat{P}_h^{DISP}\right) \qquad (23)$$

Every day, the final value of the droop results to be:

$$d_p = \min\left(d_p^D, d_p^P\right) \qquad (24)$$

4.2. Hourly offset discharge (OFF)

The second objective of the framework is to ensure the discharge set-point to be satisfied, while minimising the wear and tear of the HPP unit. Ideally, the target is to implement a single action (offset discharge) able to bring the CDE to 0. To achieve this objective, the error of the previous period and the forecast of the discharge needed to perform FCR in the following interval are computed. To this end, we can rearrange (19) as follows:

$$\Delta V_h^{OFF} = -\left(\Delta V_{h-1} + \frac{d_p}{K_h}\hat{W}_{f,h}\right) \qquad (25)$$

To minimise the number of movements of guide vanes and blades, the ΔV_h^{OFF} is given by a discharge offset that is constant over the duration T of the hour, so that the offset function causes only one movement of the governing system at the beginning of the interval and not a continuous action characterised by multiple movements over the period. As a consequence:

$$Q_h^{OFF} = \frac{\Delta V_h^{OFF}}{T} \qquad (26)$$

A graphical representation of the offset function impact on the discharge error can be seen in Fig. 5.

By considering the initial value of ΔV_h as contained within the limits ($\pm \Delta V_{max}$), the forecasting tool predicts the value of $\hat{W}_f$ which is converted into the predicted cumulative discharge deviation for FCR provision $\Delta \hat{V}_h^{FCR}$ according to (15). In Fig. 5, the light grey area represents the confidence interval of the prediction. As it is visible, without any action in terms of offset function, there is a consistent portion of the confidence interval which exceeds the limit ΔV_{max} (dark grey area in Fig. 5a). As defined in (19) the offset function equals ΔV_{h-1} plus the prediction $\Delta \hat{V}_h^{FCR}$ to centre the confidence interval in 0. By operating this control action at every period, the error is limited within $\pm \Delta V_{max}$, chosen a priori by the power plant owner, in accord with the river authority.
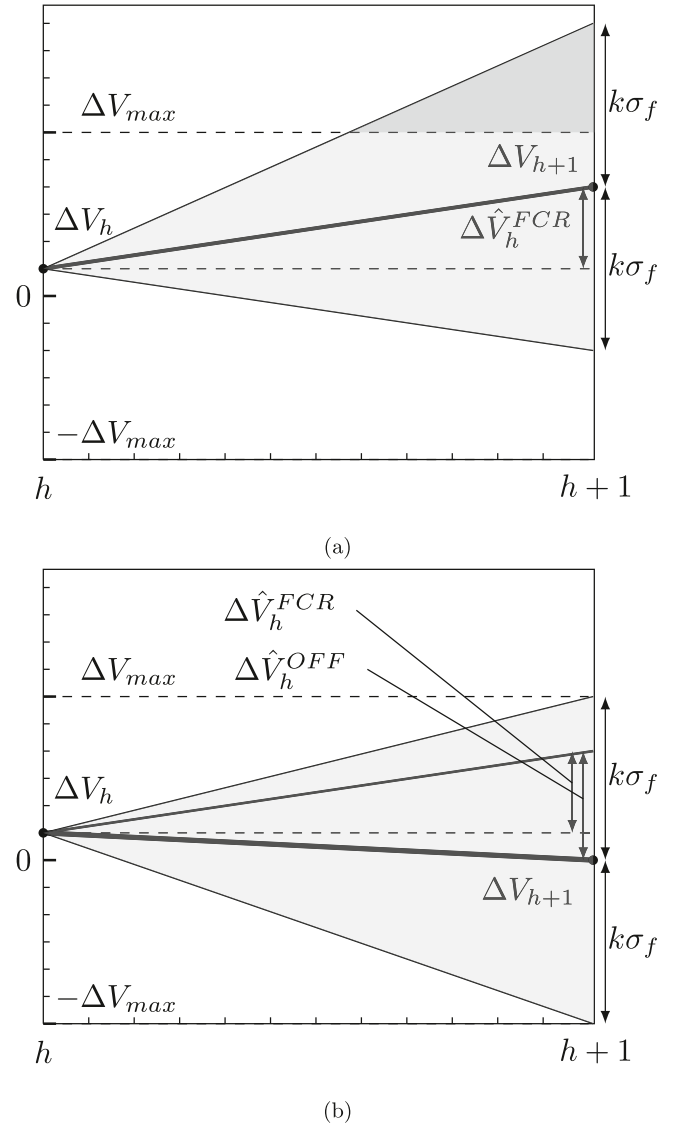

(a)

(b)

Fig. 5. Expected trajectories of the CDE due to FCR provision a period T (a) without and (b) with the action of the offset discharge Q_h^{OFF}.

4.3. Real-time optimal control (OPT)

The lowest level of control, interacting directly with the HPP, as shown in Fig. 2, takes as input the droop calculated in Section 4.1 and the offset computed in Section 4.2. This subsection is specifically addressing the control problem for double-regulated units. It can be neglected in case of applications to any RoR HPPs controlled in power and equipped with single regulated turbines.

The discharge set-point Q_h^{DISP} from the dispatch plan is summed with Q_h^{OFF} and with the discharge deviation given by the droop-controlled FCR action Q_s^{FCR}.

$$Q_s^{SET} = Q_h^{DISP} + Q_h^{OFF} + Q_s^{FCR} \qquad (27)$$

with

$$Q_s^{FCR} = \frac{\Delta f_s \cdot d_p}{\rho g H_s \eta_s} \qquad (28)$$

where the values of η_s and H_s are approximated with η_{s-1} and H_{s-a}. The term Δf_s is the frequency deviation $50 - f_s$.

Similarly to [36], the control problem can be stated as: *For a given discharge set-point Q^{SET} and external condition n_{ED} (i.e. head*

H and rotational speed *n*) find the combination of guide vanes and blades opening angles that maximises the efficiency. Every second *s*, given the measures of head H_s, rotational speed n_s and guide vanes and blades position in the previous second $\alpha_{s-1}, \beta_{s-1}$, the mathematical formulation of the problem uses as objective function a weighted sum of two contributions, ensuring the best efficiency operation and the discharge tracking as in (29):

$$\min_{\alpha,\beta} \quad \omega_1 \cdot \left[1 - \eta^*(\alpha, \beta, n_{ED,s}) \right] +$$
$$\omega_2 \cdot \left[Q_s^{SET} - Q^*(\alpha, \beta, n_{ED,s}) \right]^2 \tag{29}$$
$$\text{s.t.} \quad \alpha, \beta \in \Omega_{\alpha,\beta}$$
$$\alpha_{s-1} + v_{\alpha_c} \Delta t \leq \alpha \leq \alpha_{s-1} + v_{\alpha_o} \Delta t$$
$$\beta_{s-1} + v_{\beta_c} \Delta t \leq \beta \leq \beta_{s-1} + v_{\beta_o} \Delta t$$

where $\Delta t = 1\,s$, and $v_{\alpha_o}, v_{\alpha_c}$ are respectively the normalised maximum speeds in opening and closing of the servomotor acting on the guide vanes. The quantities v_{β_o}, v_{β_c} are the corresponding quantities for the blades servomotor. The two weights ω_1, ω_2 are chosen to, first, comply with the discharge set-point and, secondly, maximise the efficiency. Nevertheless, the choice of the weights is user dependent and beyond the scope of this paper. Constraints $\Omega_{\alpha,\beta}$ ensure that the operation is within feasible positions of guide vanes and blades. Finally, the last two constraints consider the maximum speed of the servomotors, to avoid changes in the moving organs which are physically impossible, because of a finite servomotor speed. Problem (29) is convex if:

1. $\eta^*(\alpha, \beta, n_{ED,s})$ is concave;
2. $Q^*(\alpha, \beta, n_{ED,s})$ is linear.

In the following subsections, a way to identify the validity of the first condition and to ensure the second one is proposed.

4.3.1. Concavity check of η^*

If η^* has the characteristic of been concave over all the *Operating Range* (OR), its opposite is convex, and so is the first term of the objective function. Generally, efficiency models of hydraulic turbines have a hill-like shape, usually called *hill-chart*. This characteristic supports the hypothesis of concavity, even though it does not prove it mathematically. In this regards, the well-known *Second-Order Condition* (SOC) for concavity [37] is considered. The SOC allows proving the concavity of a function by analysing its Hessian. By construction, η^* and Q^* are twice differentiable. Moreover, the guide vane opening angle α and the blade opening angle β are limited in the intervals:

$$\alpha \in [\alpha_{min}, \alpha_{max}]$$
$$\beta \in [\beta_{min}, \beta_{max}] \tag{30}$$

By normalising α and β, it is trivial to prove that:

$$\textbf{dom} \quad \eta^* = \textbf{dom} \quad Q^* = \Omega_{\alpha,\beta} = [0\,;\,1] \tag{31}$$

is convex. Therefore, it is possible to determine whether η^* is a concave function by proving that:

$$\nabla^2 \eta^*(\alpha, \beta, n_{ED}) \preceq 0 \qquad \forall \alpha, \beta \in \Omega_{\alpha,\beta} \tag{32}$$

for each given value of n_{ED} (i.e. for each given value of *H* if *n* is fixed to the synchronous rotational speed). It is possible to reformulate (32) as follows:

$$\zeta_\eta = \zeta_\eta(\alpha, \beta) = \max_{i=1}^{2} \lambda_i(\nabla^2 \eta^*(\alpha, \beta, \hat{n}_{ED})) \leq 0 \tag{33}$$

where $\lambda_{1,2}(\alpha, \beta)$ are the two eigenvalues of the matrix, and ζ is its spectral abscissa. If (33) is satisfied, for every head and rotational speed value, then $\eta^*(\alpha, \beta, n_{ED})$ is concave.

4.3.2. Linearity of Q^*

The function Q^* is built as indicated in Section 3, as a sum of piece-wise polynomials of different orders. To reach good accuracy of the discharge model, it is probable for the polynomials composing Q^* to be non-linear, as indicated in [23]. Nevertheless, when applying (29), the constraints related to the servomotors speed are forcing the solution α, β to be close to $\alpha_{s-1}, \beta_{s-1}$. Therefore, at every second *s*, Q^* can be seen as a relatively small deviation from $Q^*(\alpha_{s-1}, \beta_{s-1}, n_{ED,s})$. Since the turbine discharge is a smooth function of H, α and β, usually represented with low-order polynomia [23,24,26], it is possible to linearise Q^* around $\alpha_{s-1}, \beta_{s-1}$, indicated in this paper with the term $\overline{Q}^*(\alpha, \beta, n_{ED,s})|_{\alpha_{s-1}, \beta_{s-1}}$. The linearised form can be substituted in the second term of the objective function of (29), obtaining:

$$\omega_2 \cdot \left[Q_s^{SET} - \overline{Q}^*(\alpha, \beta, n_{ED,s})|_{\alpha_{s-1}, \beta_{s-1}} \right]^2 \tag{34}$$

If (34) is inserted in (29) as visible in (35), and (33) is satisfied, then (35) is a convex optimisation problem.

$$\min_{\alpha,\beta} \quad \omega_1 \cdot \left[1 - \eta^*(\alpha, \beta, n_{ED,s}) \right] +$$
$$\omega_2 \cdot \left[Q_s^{SET} - \overline{Q}^*(\alpha, \beta, n_{ED,s})|_{\alpha_{s-1}, \beta_{s-1}} \right]^2 \tag{35}$$
$$\text{s.t.} \quad \alpha, \beta \in \Omega_{\alpha,\beta}$$
$$\alpha_{s-1} + v_{\alpha_c} \Delta t \leq \alpha \leq \alpha_{s-1} + v_{\alpha_o} \Delta t$$
$$\beta_{s-1} + v_{\beta_c} \Delta t \leq \beta \leq \beta_{s-1} + v_{\beta_o} \Delta t$$

This formulation allows the control problem to output the global optima by applying any kind of gradient-based or interior point solver.

5. Results

In this Section, a validation of the method is presented and the performances of the framework are evaluated by numerical simulations in the Matlab environment. The simulation results are compared with measured data of the full-size RoR HPP Vogelgrun, owned by *Électricité de France* (EDF), on the Rhine river (France). The plant, commissioned in 1959, features 4 units, rating 39 MW each, for head values going from 10.5 m, to 12.5 m. Unit 1 is selected to be part of this study, and, therefore, efficiency and discharge of this unit have to be modelled as a function of the measurable variables. The simulation is built with the following characteristics:

(i) The simulation time is one month, starting from April 15, 2020, with a time sampling rate of 1 min.[2]
(ii) Every day, the computation of the droop for the following day is performed, based on the information of the day-ahead dispatch.
(iii) Every hour, the discharge set-point offset is computed based on the frequency information of the previous 8 h, as required by the AR model for the forecast of W_f.
(iv) Every minute, a new operating point is chosen for the turbine by the optimisation problem.[3]

---

[2] Length and sampling rate of the simulation are chosen based on the richest data-set available for the considered power plant.

[3] The sampling for the operation point is chosen based on the state of the art controller in the considered power plant, a faster control could be implemented, as the problem formulation allows for a fast resolution.

5.1. Surrogate model

The turbine behaviour is described by (6) and (7). Both efficiency and discharge are modelled as the sum of piece-wise cubic spline by implementing the multivariate regression method described in Section 3. The data-set used to train the algorithm is built by collecting the turbine characteristics curves data. The fitting performances are estimated by computing the *Coefficient of Determination* R^2. Both the efficiency ($R^2 = 0.9884$) and the discharge ($R^2 = 0.9992$) surrogate models obtain excellent results. Moreover, the models are validated over one-month operation time history data of Vogelgun RoR HPP. For every second of the day, the measured values of α, β, H, n contained in the SCADA are acquired, the power of the HHP is computed as:

$$P = \rho \cdot g \cdot H \cdot Q^*(\alpha, \beta, n_{ED}) \cdot \eta^*(\alpha, \beta, n_{ED}) \qquad (36)$$

and compared with the measured active power. The error between calculated and measured power is contained between $\pm 2.4\%$ in 95% of the cases and between $\pm 4\%$ in 99.5% of the cases. This proves the analytical function to be accurate and supports the choice of representing the system only with its static behaviour described by (2) and (3).

Moreover, the error introduced by the linearisation of Q has been estimated. As previously mentioned in Section 4.3.2, the linearisation of Q should not introduce a considerable error for two reasons:

- the turbine discharge is a smooth function of H, α and β, usually represented with low-order polynomia [23,24,26]
- the servomotors controlling α and β are subject to hard limitation in the movements, in terms of maneuvering speed.

The numerical proof of the above statement is given here below for the turbine object of the study. A mapping of the *Root-Mean-Square Error* (RSME) and the *Coefficient of Determination* (R^2) over the entire domain is visible in Fig. 6. Moreover, the statistical quantities *Cumulative Density Function* (CDF) and *Probability Density Function* (PDF) for R^2 are shown in Fig. 7. All the indicators have been computed by considering 10000 points equally distributed in the feasible region $\Omega_{\alpha,\beta}$. Both the indicators (RMSE ≤ 0.2 and $R^2 \geq 0.99$) demonstrate that the linearisation can be considered as feasible for control purposes.

A further step is made to assess the concavity of η^*. To obtain a mathematical proof of the concavity of η^*, (33) is considered. Fig. 8 shows in blue the portion of $\Omega_{\alpha,\beta}$ where ζ_η is ≤ 0, for a head value of $\hat{H} = 12$ m, and, therefore, where η^* can be considered concave. For every discharge value (i.e. for every discharge iso-line) the optimisation algorithm is responsible for choosing the best combination of α and β, that maximises efficiency. The hypothesis of concavity does not hold on the border between the blue and the red region. It can be proven that the red region is concave, hence the optimal solution is reached for discharge iso-lines entirely falling in this area. Nevertheless, for the discharge iso-lines crossing region, the optimisation problem will select a local minimum. A similar result is obtained for other head values. Since the non-convex area represents only a small portion of the domain, this does not drastically affect the result.

5.2. Control strategy validation

5.2.1. Droop computation

The method presented in Section 4.1 proposes that the daily droop should correspond to the minimum value between:

- The droop d_p^D, based on the maximum admissible CDE.
- The droop d_p^P, compatible with the turbine power rating.

Table 2
Droop coefficient values [kW/Hz], EPFL database.

	γ	K_d with H_{min}	K_d with H_{avg}
d_p^D	95%	20415	21275
	99%	15553	16162
d_p^P	95%	56746	79246
	99%	56746	79246
Current frequency droop in the HPP of Vogelgrun $d_p = 17500$			

According to (21), it is necessary to estimate the conversion factor K_d to compute the maximum droop coefficient d_p^D. Since the choice has to be made every day for the following one, the estimation of K_d has to be made based on the day-ahead dispatch. The value of K_d depends on the quantities H_d and η_d, according to (16). To compute these quantities, the following approach is considered: a probability density function of the head values over one year is computed and, by considering a confidence interval of 95%, the minimum head $\hat{H}_{min}$ is considered to compute K_d. The estimation of η_d is made by knowing the discharge set-point from the day-ahead dispatch and by considering $\hat{H}_{min}$ as the head for the day after. This approach allows making the optimisation more robust since the choice of $\hat{H}_{min}$ as reference head for the calculation leads to the computation of a lower value of maximum droop. The achieved results are compared with the estimation of η_d where the average value of head $\hat{H}_{avg}$ is considered. The results, for two different CI for the frequency forecaster and two different approaches in the computation of the conversion factor K_d are compared in Table 2. For the computation of these droops, the chosen value for the maximum admissible error ΔV_{max} is 9000 m^3, corresponding to 1% of the total amount of water flowing through one unit, in one hour, when the unit operates with a constant discharge value of 250 m^3/s.

During the month of analysis, the discharge set-points are not close to the maximum value of discharge of the HPP. As a consequence, by looking at Table 2, it is possible to observe that the droop d_p^P, computed according to (22), is always greater than d_p^D and, therefore, this latter is adopted. In all cases, the optimally determined droop is higher than the corresponding value given by state of the art approaches.

5.2.2. Discharge management validation

Four scenarios (two different CIs in the forecasting tools and two different approaches in the computation of K_d) are simulated and compared in terms of reliability, to test the algorithm robustness. A graphical representation of the results for the less robust case (CI= 95% and K_d computed with $\hat{H}_{avg}$), is given in Fig. 9. The CDE is shown in bold red for 12 of the 720 simulated hours. It is possible to observe the predicted discharge error due to FCR action $\Delta \hat{V}_i^{FCR}$ and the relative action $\Delta \hat{V}_i^{OFF}$ of the control. Every hour, the estimation $\Delta \hat{V}_i^{FCR}$ is computed. The offset function $\Delta \hat{V}_i^{OFF}$ is calculated according to (19). It is noticed that, without the offset function calculated in the discharge management framework, the error ΔV would increase and get greater than the limits, as highlighted in Fig. 9 by the red thin curve. The direct consequence would be that, over time, the head of the river would deviate from the expected one, since the power plant is operating with a different discharge value. By applying the framework, the error is contained within the limits ($\pm 1\%$). Furthermore, the discharge is controlled just by acting on guide vanes and blades opening angle once per hour, i.e. limiting the number of movements due to discharge management. This represents a noticeable improvement compared to state of the art controls adopted for the operation of RoR HPP, where the discharge is re-adjust every minute to minimise the error due to frequency
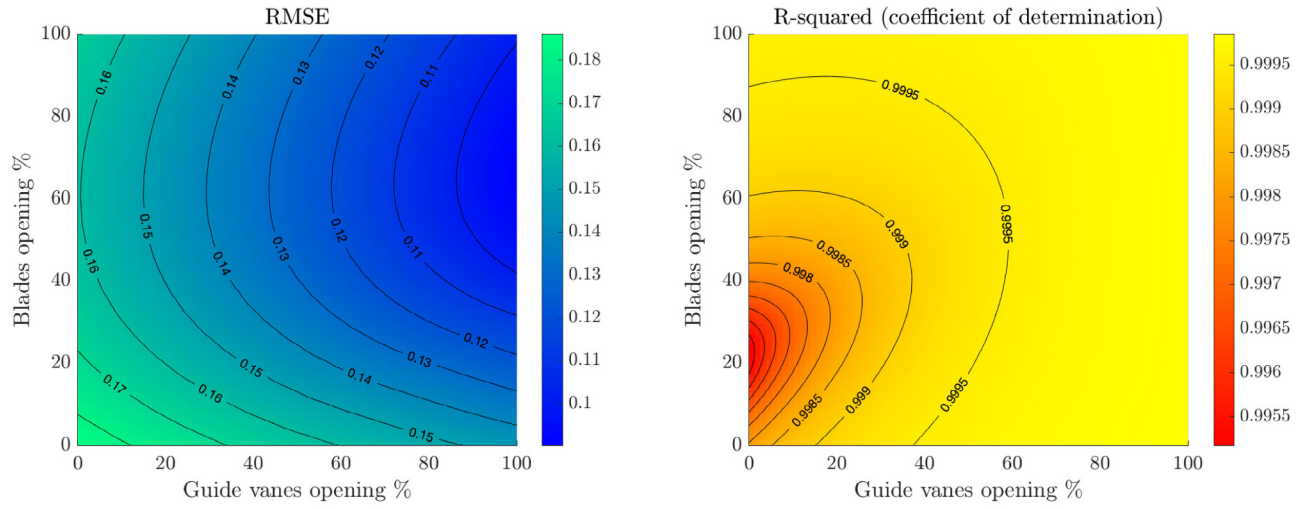
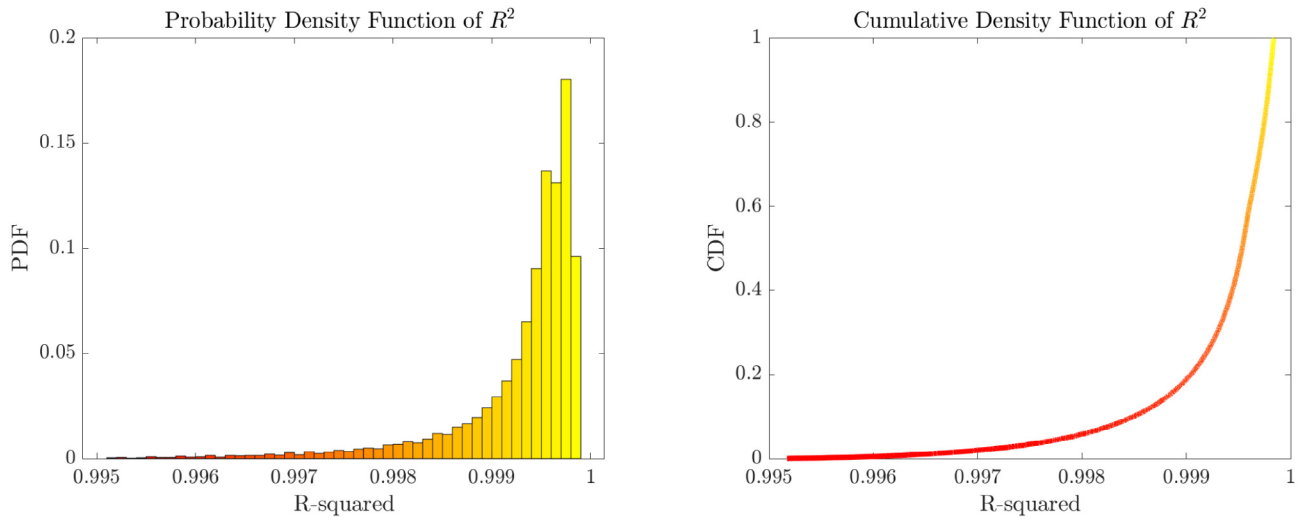**Fig. 6.** RMSE and R^2 of the linearisation mapped over all the operation points.

Fig. 7. Probability density function and cumulative density function of the linearisation R^2.
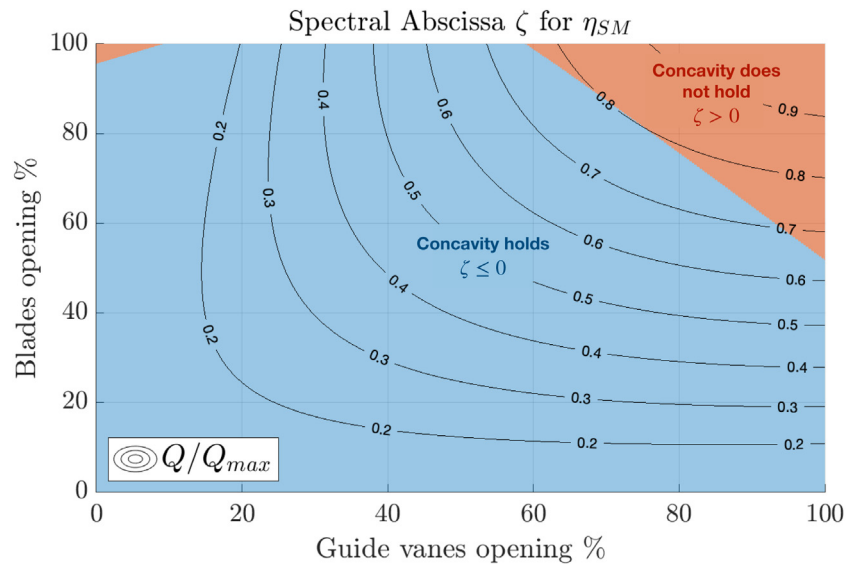

Fig. 8. Space of solutions for (33) for $\hat{H} = 12\ m$. The contour lines represent different discharge levels, normalised with respect to their maximum value. (For interpretation of the references to colour in this figure legend, the reader is referred to the web version of this article.)
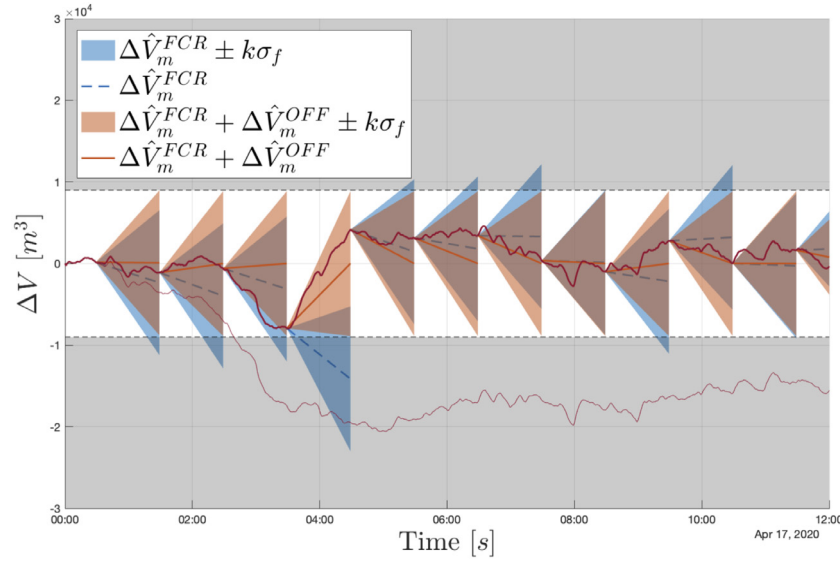
Fig. 9. Comparison of predicted value $\Delta\hat{V}_h^{FCR}$, the offset function $\Delta\hat{V}_h^{OFF}$ and the CDE in bold-red. In light-red the scenario with enhanced droop but without discharge management.

Table 3
λ_T for different strategies.

	γ	K_d with H_{min}	K_d with H_{avg}
λ_T	95%	98.18%	97.70%
	99%	99.74%	99.67%

control. To assess the performances of the proposed framework, the term λ_T can be defined as *the duration of the period in which the discharge error is within the limit ΔV_{max}, expressed in percentage of the simulation duration*. Table 3 shows the values of λ_d for the different approaches, while the droop computation is shown in Table 2. For the case considering K_d with H_{avg}, the proposed framework is able to enhance the droop, obtaining an average value over 30 days that corresponds to 121% of the value obtained by state of the art operational practices in the HPP of Vogelgrun. Despite the increase of FCR provision, the discharge of the RoR HPP is managed by operating just one movement per hour and by containing the discharge error within $\pm 1\%$ for 97.70% of the time, within $\pm 1.5\%$ in 99.85% of the time and between $\pm 2.2\%$ during the whole simulation.

5.2.3. Validation of the real time optimal control
The latter layer of the framework, to be applied in case of double-regulated turbines, consists in the computation of α and β by Eq. (35), given a certain discharge set-point, defined in Eq. (27). The solution is found by taking advantage of the Yalmip toolbox coupled with `fmincon` solver, in the Matlab environment. Without considering the effect of the last two constraints, it can be proved that the choice of α and β given by Eq. (35) coincides with the output of the general gate-dominant control, where the relation between α and β is defined by the CAM block lookup table. This result is supported by [38], where the decoupling of guide vanes and blades control is proved to outperform the gate-dominant control just in high transient conditions, such as load rejections, which are not treated in this study. Furthermore, based on the existing literature, it can be expected the wear and tear to be reduced. As indicated in [39], when performing FCR provision Kaplan units may be operating slightly off-cam since the blades regulating mechanism is slower and lags behind the guide vanes regulating mechanism. Since Eq. (35) takes as input already the discharge set-point that includes FCR, it is able to propose a solution for α and β that respects the servomotors speeds and maximises the efficiency. As stated in [12], the efficiency loss due to off-cam operation due to FCR provision is almost negligible, but its effect on the wear reduction strategies is not. Therefore, it is not possible to state that the optimisation problem represents an improvement in terms of efficiency, with respect to the gate-dominant approach, but still it leads to a reduction in the wear and tear originated by FCR provision. Moreover, the proposed optimal control is formulated in order to be integrated with additional information, such as wear and tear estimation, that steer the optimisation towards the maximisation of multiple objectives.

6. Conclusion

A droop-based control framework to enhance FCR provision with a RoR HPP has been presented. The computation of the droop coefficient and the discharge management rely on the forecast of the energy required for FCR provision over a time horizon of one hour, performed by AR models. It has been shown that, by considering the information provided by such forecasts, the HPP control can provide more regulating power while ensuring the system reliability in terms of discharge control. The discharge deviation from the set-point, caused by the provision of flexibility, is controlled by computing an offset discharge once per hour which, therefore, reduces the number of movements of the regulating components of the hydroelectric unit. This constitutes an improvement for the standard control system that imposes continuous movements of guide vanes and blades to respect the discharge set-point. Furthermore, the real-time control is formulated as a convex optimisation problem, able to calculate the best combination of guide vanes and blades opening angles for maximising the efficiency. The proposed method is validated via numerical simulations. Further studies will be implemented to include in the optimisation problem also critical system conditions such as fatigue and wear and tear of the components. Validation on a reduced scale model will be performed to confirm the performances of the complete framework.

CRediT authorship contribution statement

F. Gerini: Conceptualisation, Methodology, Writing – original draft, Software. **E. Vagnoni:** Data curation, Writing – review & editing. **R. Cherkaoui:** Supervision. **M. Paolone:** Supervision, Project administration.

Declaration of competing interest

The authors declare that they have no known competing financial interests or personal relationships that could have appeared to influence the work reported in this paper.

Acknowledgements

References

[1] E. N. of Transmission System Operators for Electricity, ENTSO-E Statistical Factsheet, Tech. Rep., ENTSO-E, 2019.

[2] A. Padoan, C. Nicolet, B. Kawkabani, J.-J. Simond, A. Schwery, F. Avellan, Stability study of a mixed islanded power network, in: 2010 IEEE/PES Transmission and Distribution Conference and Exposition: Latin America (T & D-LA), IEEE, Sao Paulo, Brazil, 2010, pp. 218–225, http://dx.doi.org/10.1109/TDC-LA.2010.5762885, URL http://ieeexplore.ieee.org/document/5762885/.

[3] L.I. Levieux, F.A. Inthamoussou, H. De Battista, Power dispatch assessment of a wind farm and a hydropower plant: A case study in Argentina, Energy Convers. Manag. 180 (2019) 391–400, http://dx.doi.org/10.1016/j.enconman.2018.10.101, URL https://linkinghub.elsevier.com/retrieve/pii/S0196890418312299.

[4] J. Zhang, C. Cheng, S. Yu, H. Wu, M. Gao, Sharing hydropower flexibility in interconnected power systems: A case study for the China Southern power grid, Appl. Energy 288 (2021) 116645, http://dx.doi.org/10.1016/j.apenergy.2021.116645, URL https://linkinghub.elsevier.com/retrieve/pii/S0306261921001781.

[5] H. Villegas Pico, J. McCalley, Modeling and analysis of speed controls in hydro-turbines for frequency performance, in: 2011 North American Power Symposium, IEEE, Boston, MA, USA, 2011, pp. 1–7, http://dx.doi.org/10.1109/NAPS.2011.6024847, URL http://ieeexplore.ieee.org/document/6024847/.

[6] Z. Zhao, J. Yang, W. Yang, J. Hu, M. Chen, A coordinated optimization framework for flexible operation of pumped storage hydropower system: Nonlinear modeling, strategy optimization and decision making, Energy Convers. Manag. 194 (2019) 75–93, http://dx.doi.org/10.1016/j.enconman.2019.04.068, URL https://linkinghub.elsevier.com/retrieve/pii/S0196890419305023.

[7] B. Hase, C. Seidel, Balancing services by run-of-river-hydropower at low reservoir amplitudes: Potentials, revenues and emission impacts, Appl. Energy 294 (2021) 116988, http://dx.doi.org/10.1016/j.apenergy.2021.116988, URL https://linkinghub.elsevier.com/retrieve/pii/S0306261921004578.

[8] Sánchez Platero, Allenbach Nicolet, Hydropower plants frequency regulation depending on upper reservoir water level, Energies 12 (9) (2019) 1637, http://dx.doi.org/10.3390/en12091637, URL https://www.mdpi.com/1996-1073/12/9/1637.

[9] W. Yang, P. Norrlund, L. Saarinen, J. Yang, W. Guo, W. Zeng, Wear and tear on hydro power turbines – Influence from primary frequency control, Renew. Energy 87 (2016) 88–95, http://dx.doi.org/10.1016/j.renene.2015.10.009, URL https://linkinghub.elsevier.com/retrieve/pii/S0960148115303621.

[10] G. Lazzaro, S. Basso, M. Schirmer, G. Botter, Water management strategies for run-of-river power plants: Profitability and hydrologic impact between the intake and the outflow: Hydroeconomic Performances of Water Management Strategies, Water Resour. Res. 49 (12) (2013) 8285–8298, http://dx.doi.org/10.1002/2013WR014210, URL http://doi.wiley.com/10.1002/2013WR014210.

[11] G. Robert, F. Michaud, A simple multi-objective control for cascaded hydro power plants, IFAC Proc. Vol. 44 (1) (2011) 4960–4963, http://dx.doi.org/10.3182/20110828-6-IT-1002.00654, URL https://linkinghub.elsevier.com/retrieve/pii/S1474667016443922.

[12] W. Yang, P. Norrlund, L. Saarinen, A. Witt, B. Smith, J. Yang, U. Lundin, Burden on hydropower units for short-term balancing of renewable power systems, Nat. Commun. 9 (1) (2018) 2633, http://dx.doi.org/10.1038/s41467-018-05060-4, URL http://www.nature.com/articles/s41467-018-05060-4.

[13] M. Zhang, D. Valentín, C. Valero, M. Egusquiza, E. Egusquiza, Failure investigation of a Kaplan turbine blade, Eng. Fail. Anal. 97 (2019) 690–700, http://dx.doi.org/10.1016/j.engfailanal.2019.01.056, URL https://linkinghub.elsevier.com/retrieve/pii/S1350630718309191.

[14] W. Yang, P. Norrlund, J. Yang, Analysis on regulation strategies for extending service life of hydropower turbines, IOP Conf. Ser.: Earth Environ. Sci. 49 (2016) 052013, http://dx.doi.org/10.1088/1755-1315/49/5/052013, URL https://iopscience.iop.org/article/10.1088/1755-1315/49/5/052013.

[15] Jiangnan Xi, H.R. Chamorro, J. Persson, A. Westberg, D. Wall, M. Ghandhari, On the influence of the backlash governor settings on the frequency response in power systems, in: 2016 IEEE PES Asia-Pacific Power and Energy Engineering Conference, APPEEC, IEEE, Xi'an, China, 2016, pp. 732–737, http://dx.doi.org/10.1109/APPEEC.2016.7779650, URL http://ieeexplore.ieee.org/document/7779650/.

[16] G. Liu, S. Daley, Optimal-tuning nonlinear pid control of hydraulic systems, Control Eng. Pract. 8 (9) (2000) 1045–1053, http://dx.doi.org/10.1016/S0967-0661(00)00042-3, URL https://linkinghub.elsevier.com/retrieve/pii/S0967066100000423.

[17] E. Çam, Application of fuzzy logic for load frequency control of hydro-electrical power plants, Energy Convers. Manag. 48 (4) (2007) 1281–1288, http://dx.doi.org/10.1016/j.enconman.2006.09.026, URL https://linkinghub.elsevier.com/retrieve/pii/S0196890406003062.

[18] C. Jin, N. Lu, S. Lu, Y. Makarov, R.A. Dougal, Coordinated control algorithm for hybrid energy storage systems, in: 2011 IEEE Power and Energy Society General Meeting, IEEE, San Diego, CA, 2011, pp. 1–7, http://dx.doi.org/10.1109/PES.2011.6039893, URL https://ieeexplore.ieee.org/document/6039893/.

[19] W. Yang, P. Norrlund, L. Saarinen, J. Yang, W. Zeng, U. Lundin, Wear reduction for hydropower turbines considering frequency quality of power systems: a study on controller filters, IEEE Trans. Power Syst. 32 (2) (2017) 1191–1201, http://dx.doi.org/10.1109/TPWRS.2016.2590504, URL https://ieeexplore.ieee.org/document/7514942/.

[20] M. Intelligence, Europe Hydro Turbine Market - Growth, Trends, Covid-19 Impact, and Forecasts (2021 - 2026), Tech. Rep., 2021, URL https://www.mordorintelligence.com/industry-reports/europe-hydro-turbine-market.

[21] H.G. Hansson, Development of the Kaplan Turbine 28.

[22] A. Borghetti, M.D. Silvestro, G. Naldi, M. Paolone, M. Alberti, Maximum efficiency point tracking for adjustable-speed small hydro power plant, 2008, p. 7.

[23] M. Brezovec, I. Kuzle, T. Tomisa, Nonlinear digital simulation model of hydroelectric power unit with kaplan turbine, IEEE Trans. Energy Convers. 21 (1) (2006) 235–241, http://dx.doi.org/10.1109/TEC.2005.847963, URL http://ieeexplore.ieee.org/document/1597342/.

[24] H.A. Menarin, H.A. Costa, G.L.M. Fredo, R.P. Gosmann, E.C. Finardi, L.A. Weiss, Dynamic modeling of kaplan turbines including flow rate and efficiency static characteristics, IEEE Trans. Power Syst. 34 (4) (2019) 3026–3034, http://dx.doi.org/10.1109/TPWRS.2019.2899815, URL https://ieeexplore.ieee.org/document/8642905/.

[25] D. Kosterev, Hydro turbine-governor model validation in pacific northwest, IEEE Trans. Power Syst. 19 (2) (2004) 1144–1149, http://dx.doi.org/10.1109/TPWRS.2003.821464, URL http://ieeexplore.ieee.org/document/1295026/.

[26] J. Zhao, L. Wang, D. Liu, J. Wang, Y. Zhao, T. Liu, H. Wang, Dynamic model of kaplan turbine regulating system suitable for power system analysis, Math. Probl. Eng. 2015 (2015) 1–12, http://dx.doi.org/10.1155/2015/294523, URL http://www.hindawi.com/journals/mpe/2015/294523/.

[27] E. Vagnoni, L. Andolfatto, S. Richard, C. Münch-Alligné, F. Avellan, Hydraulic performance evaluation of a micro-turbine with counter rotating runners by experimental investigation and numerical simulation, Renew. Energy 126 (2018) 943–953, http://dx.doi.org/10.1016/j.renene.2018.04.015, URL https://linkinghub.elsevier.com/retrieve/pii/S0960148118304233.

[28] J.H. Friedman, Multivariate adaptive regression splines, Ann. Statist. 19 (1) (1991) http://dx.doi.org/10.1214/aos/1176347963, URL https://projecteuclid.org/journals/annals-of-statistics/volume-19/issue-1/Multivariate-Adaptive-Regression-Splines/10.1214/aos/1176347963.full.

[29] C. Vessaz, L. Andolfatto, F. Avellan, C. Tournier, Toward design optimization of a pelton turbine runner, Struct. Multidiscip. Optim. 55 (1) (2017) 37–51, http://dx.doi.org/10.1007/s00158-016-1465-7, URL http://link.springer.com/10.1007/s00158-016-1465-7.

[30] E. Vagnoni, L. Andolfatto, R. Guillaume, P. Leroy, F. Avellan, Interaction of a rotating two-phase flow with the pressure and torque stability of a reversible pump-turbine operating in condenser mode, Int. J. Multiph. Flow 111 (2019) 112–121, http://dx.doi.org/10.1016/j.ijmultiphaseflow.2018.11.013, URL https://linkinghub.elsevier.com/retrieve/pii/S0301932218302763.

[31] Regelleistung website, URL https://www.regelleistung.net.

[32] I. Laura, Terms and conditions for providers of frequency containment reserves (FCR), 2019, p. 19, URL https://www.fingrid.fi/globalassets/dokumentit/en/electricity-market/reserves/fcr-liite1---ehdot-ja-edellytykset_en.pdf.

[33] G. Piero Schiapparelli, S. Massucco, E. Namor, F. Sossan, R. Cherkaoui, M. Paolone, Quantification of primary frequency control provision from battery energy storage systems connected to active distribution networks, in: 2018 Power Systems Computation Conference, PSCC, IEEE, Dublin, 2018, pp. 1–7, http://dx.doi.org/10.23919/PSCC.2018.8442554, URL https://ieeexplore.ieee.org/document/8442554/.

[34] M. Pignati, M. Popovic, S. Barreto, R. Cherkaoui, G. Dario Flores, J.-Y. Le Boudec, M. Mohiuddin, M. Paolone, P. Romano, S. Sarri, T. Tesfay, D.-C. Tomozei, L. Zanni, Real-time state estimation of the EPFL-campus medium-voltage grid by using PMUs, in: 2015 IEEE Power & Energy Society Innovative Smart Grid Technologies Conference, ISGT, IEEE, Washington, DC, USA, 2015, pp. 1–5, http://dx.doi.org/10.1109/ISGT.2015.7131877, URL http://ieeexplore.ieee.org/document/7131877/.

[35] E. Namor, Advanced Models and Algorithms to Provide Multiple Grid Services with Battery Storage Systems, EPFL, Lausanne, 2018, http://dx.doi.org/10.5075/EPFL-THESIS-8734, URL http://infoscience.epfl.ch/record/256959.

[36] F. Gerini, E. Vagnoni, R. Cherkaoui, M. Paolone, Optimal CAM computation of kaplan turbines accounting for wear and tear originated by frequency control, in: 2021 IEEE Madrid PowerTech, IEEE, Madrid, Spain, 2021, pp. 1–6, http://dx.doi.org/10.1109/PowerTech46648.2021.9495080, URL https://ieeexplore.ieee.org/document/9495080/.

[37] S.P. Boyd, L. Vandenberghe, Convex optimization, Cambridge University Press, Cambridge, UK, New York, 2004.

[38] P. Schniter, L. Wozniak, Efficiency based optimal control of Kaplan hydrogenerators, IEEE Trans. Energy Convers. 10 (2) (1995) 348–353, http://dx.doi.org/10.1109/60.391902, URL http://ieeexplore.ieee.org/document/391902/.

[39] L. Saarinen, P. Norrlund, W. Yang, U. Lundin, Allocation of frequency control reserves and its impact on wear and tear on a hydropower fleet, IEEE Trans. Power Syst. 33 (1) (2018) 430–439, http://dx.doi.org/10.1109/TPWRS.2017.2702280, IEEE Transactions on Power Systems.